Multidisciplinary Aircraft Design and Trajectory Control Optimization

Lourenço Lúcio
lourenco.lucio@tecnico.ulisboa.pt

Instituto Superior Técnico, Lisboa, Portugal

December 2019

Abstract

In the pursuit of increasing aircraft performance, one approach which can yield better results than a conventional design process is a multidisciplinary optimization process. In this paradigm, a design architecture is established so that the analyses for the several disciplines pertinent to the problem are handled simultaneously, rather than sequentially. In this work, a numerical tool was developed in order to perform low-fidelity multidisciplinary optimization upon a commercial airliner - the *B777-300* - considering models for aerodynamics, propulsion, structures and trajectory. For the aerodynamic analysis, a vortex-lattice method (VLM) is employed. The lifting surface structures were modeled by finite elements with the shape of hollow tubular spars. For the propulsion system, a model based on empirical data collected from the target engines was utilized. Finally, the system was optimized for cruise conditions, and then control optimization was performed on the resulting configuration for additional mission phases. The performance metric optimized in this work was be the amount of fuel burnt by the aircraft in order to complete its mission. The described optimization processes were successfully carried out, the former outputting the cruise-optimized wing and tail configurations, and the latter providing the optimized control parameter values for descent flight conditions. These values were validated by means of comparison with those of the original *B777-300*, including that of the performance metric - which improved as more disciplines were considered.

Keywords: Multidisciplinary optimization, Trajectory control optimization, Aerostructural optimization, Vortex lattice method, Finite element method

1. Introduction

With the consistently increasing demand for commercial flights, the rate of fuel burn of the employed aircraft has been a metric of great interest for several decades. Some modern approaches have been, for example, the possibility of hybrid and electric aircraft or the research of more exotic configurations such as the blended wing-body design [1]. A field of great interest in assessing the possibilities of these new configurations as well as improving the currently available aircraft has been Multidisciplinary Design Analysis and Optimization (MDAO). In an MDAO-based framework, the main goal is to take into account several disciplines of the aircraft development and usage during the design process simultaneously.

Historically, the design process of an aircraft would be approached in a multiple team system, where each one would focus on a specific area of expertise - control, aerodynamics, noise, etc. These areas and their respective analyses, however, are tightly coupled; rendering a sequential approach to the aircraft design non-optimal. An MDAO approach seeks to rectify this situation. An example of this non-optimality can be observed in fig. 1, where it can be seen that all the design points computed by the multidisciplinary approach are strictly superior to those obtained via sequential optimization. Another example of how the sequential approach is inferior to integrated aerostructural optimization is Chittick and Martins [2].

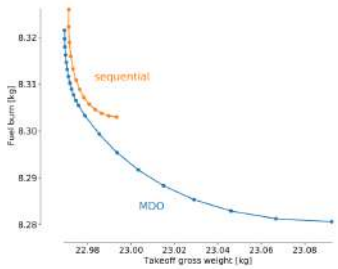

Figure 1: Comparison between Pareto fronts for sequential and multidisciplinary optimization [3].

Because every aspect of the aircraft's perfor-

mance is analytically defined as either a necessity (constraint) or that which is to be optimized (be it range, fuel burnt, lift-to-drag ratio, etc.), it is possible to ascertain whether the current design point is the optimal solution in the surrounding design space given the stipulations that are defined for what "optimal" is. A commonly used metric is the Breguet equation [4], while another possibility is to consider a composite objective [5], meaning more than one function is weighted when computing the optimality of the design.

As for the trajectory portion of the problem, it is usually worked into the optimization process through a method transverse to the discussion of disciplines and design method. Rather than adding another discipline per se to the process, be it sequential or optimized, a more common approach is to consider several flight conditions for the same current design - a multipoint approach [6].

On the implementation end, frameworks such as OpenMDAO [7] have been developed, which allows for the creation of MDAO schemes based on several data passing options within the code structure. These schemes are usually referred to as architectures, and an extensive survey on these was published by Martins and Lambe [8].

Freeware code has been developed to solve the aerostructural problem in specific in low-fidelity fashion [3]. This makes that same problem a good starting point. The motivation for this dissertation is to explore the potentiality of an MDAO approach to the aircraft design problem. To this end, the discipline of propulsion and the mission profile planning will be coupled to a preexisting MDO aerostructural code, *OpenAeroStruct* [3].

2. Background

2.1. Multidisciplinary Design Analysis and Optimization - MDAO

In this section some of the most essential concepts in MDAO are defined. The objective function surmises the fundamental goal of the whole optimization. It is the parameter that is to be minimized. A design variable is the way in which the solver is capable of changing the value of the objective function; these are the parameters of the problem which are allowed to change. Therefore, the optimization problem can be thought of as finding the set of values for the defined set of design variables which yields a minimum of the objective function. A discipline analysis defines the system of equations which describes the functioning of that same discipline in an MDO problem. State variables are the outputs of the several analyses which constitute the current state of the system (i.e., at that iteration); coupling variables constitute the state variables which are necessary for other analyses. Finally, constraints are defined so that the system yields applicable results.

The architecture of a MDAO system lays out how the data is processed, and can be graphically visualized in a eXtended Design Structure Matrix (XDSM) [9]. Fig. 2 illustrates a multidisciplinary feasible process similar to the one employed at the core of this work.

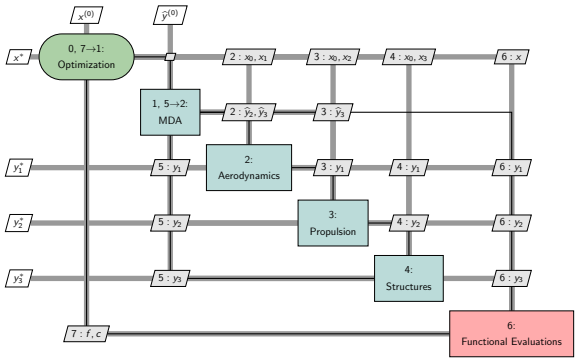

Figure 2: XDSM for a MDF architecture with a Gauss-Seidel MDA solver.

Following the sequential numeral flow in fig. 2, the MDA solver iterates through all of the discipline analyses until it converges, meaning that at every optimization iteration a consistent set of feasible coupling variables is obtained. Then, functional evaluations are carried out with these variables (computing the objective function and constraint values at that design point) and the next step is determined.

This next step is determined based on an optimization algorithm. These can be divided into zeroth order methods, also referred to as gradient-free methods; and gradient-based methods [4]. For the sake of brevity, only gradient-based methods are covered here.

These are algorithms which define a search direction in which to progress from point i to the next. The direction is based on both evaluations of the objective function and its derivatives with respect to the design parameters, meaning these solvers utilize more information in order to navigate the design space. These algorithms require smooth objective functions within the design space to operate, but then are generally faster as they require fewer function evaluations [4].

The optimization algorithm employed in this work is a sequential quadratic programming (SQP) algorithm. The idea behind SQP methods is to break down the original optimization problem (a non-linear programming problem) into a quadratic programming subproblem at design point $\boldsymbol{x}_i$. By solving this significantly simpler subproblem, one where the objective function is quadratic and the

constraints are linear functions, the algorithm then proceeds to design point $\boldsymbol{x}_{i+1}$ [10], [11].

Beside determining the next step, the computation of derivatives of quantities such as the objective function or the constraints w.r.t. the variables of the problem is an important aspect of how the problem is approached. This is what is called the sensitivity analysis, i.e., how the performance metrics of the solution are sensible to the parameters that drive the design process.

Several methods of sensitivity analysis exist, amongst which some of the most popular include complex-step derivatives or finite differences. How the sensitivity analysis is performed within a specific problem relies deeply on how data is being processed from an implementation point-of-view. In this situation, the main goal is to provide a way to compute derivatives across the several components which make up the optimization structure. Essentially, rather than just considering the impact that a given variable has on a specific function, the influence that same variable has on other state or coupled variables is also to be contemplated.

To this end, the MDAO framework utilized in this work employs a Modular Analysis and Unified Derivatives (MAUD) sensitivity analysis architecture [12]. From a practical point, the great advantage of this architecture is that for each of the logic blocks in which computations are performed, only the partial derivatives of the outputs w.r.t. the inputs for that block in specific must be defined. The assembling and computation of the full model derivatives is carried out automatically [12].

2.2. Dynamics & Equilibrium

The three equilibrium equations to be defined for longitudinal in-plane motion are the equilibrium of vertical forces, horizontal forces, and moment. The dimensional version of these equations is derived from the simplified diagram represented in fig. 3, which assumes steady flight conditions.

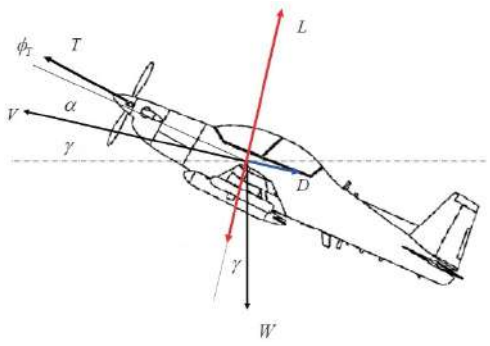

Figure 3: Free body diagram for trim.

$$L - W\cos(\gamma) + T\sin(\alpha + \phi_T) = 0 \tag{1a}$$
$$T\cos(\alpha + \phi_T) - D - W\sin(\gamma) = 0 \tag{1b}$$
$$M = 0, \tag{1c}$$

In eqs. 1a,1b and 1c, L, W, T, D and M represent the lift, total weight, thrust, drag and total moment, respectively; α, ϕ_T and γ represent the angle-of-attack, thrust incidence and flight path angle, also respectively. These equations can be broken down further, but they represent the core of the trimming conditions that will be implemented.

2.3. Aerodynamics - VLM

The vortex-lattice method (VLM) is a common low-fidelity approach to model incompressible potential flow. It is an extension of the lifting-line method [13]. A Prandtl-Glauert correction is also employed in this work given the relatively high Mach number at which the aircraft operates ($M = 0.84$). In order to enable a two-dimensional description of the lifting surfaces, several lifting-lines are superimposed along the chordwise direction. By constructing a mesh of horseshoe vortexes as such, a grid (or lattice) of control points is defined. For each of these points, a velocity $\boldsymbol{V}$ will be induced by each of the vortexes discretized. These velocities can be obtained via the Biot-Savart law,

$$d\boldsymbol{V} = \frac{\Gamma}{4\pi} \frac{\boldsymbol{dl} \times \boldsymbol{r}}{\|\boldsymbol{r}\|^3}\,, \tag{2}$$

where Γ is the circulation of the vortex, $\boldsymbol{dl}$ moves along the vortex filament at hand and $\boldsymbol{r}$ is the distance from said filament to the control point. It is then possible to assemble a system relating all the vortex circulations (Γ_n) to the induced velocities on all control points (v_n), which can be described as

$$v_n = \sum_{m=1}^{N} \{C_{n,m}\}\Gamma_m\,, \tag{3}$$

where N represents the total number of vortexes defined and $C_{n,m}$ represents a row of the aerodynamic influence coefficient (AIC) matrix. These coefficients represent the influence of each vortex on each control point. In eq. 3 the induced velocity at control point n is determined by adding the contributions of all N vortexes.

2.4. Structures

Now to define a scheme which allows the evaluation of the stiffness, $[K]$, of the structures. This will be accomplished via Hooke's Law, formulated as

$$[K] \times \boldsymbol{u} = \boldsymbol{F}\,, \tag{4}$$

where $\boldsymbol{u}$ is the displacement vector and $\boldsymbol{F}$ the force/moment vector. To this end, a finite element

method (FEM) approach is employed. At its core, what this method aims to do is break the domain (in this work, the lifting surfaces) into smaller, easier to model pieces (elements). When applying finite element methods, one of the most important decisions is which element to use. The lifting surfaces of the aircraft usually present a wingbox-type structure, with a thin-walled spar and hollow interior. Therefore, in this work a spatial beam element with 12 degrees of freedom (6 on each node) is utilized.

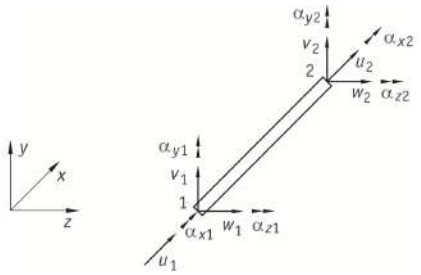

Figure 4: 12-DOF beam element.

In essence, the approach will consist of determining the element's properties at a local level (i.e. on a local reference frame) and then converting these to a global frame, obtaining the global stiffness matrix $[K]$ for the entire structure.

The aerodynamic analysis provides a set of loads, $\boldsymbol{f}$, applied to the lifting surfaces. Now that the structure's stiffness has also been defined, the aforementioned linear system (eq. 4) may be solved, yielding $\boldsymbol{u}[1 \times 12]$. This vector is the displacement and rotation vector enacting on the structure. The process may then iterate upon the architecture, computing the new set of loads applied to the updated mesh.

2.5. Propulsion Model

Several parameters are crucial in the formal definition of a jet engine, such as the number of compression stages (and respective compression ratios), duct dimensions and expansion stages or the bypass factor. The aim is to employ a generic model, capable of estimating thrust from generic parameters rather than committing to an engine type.

At its simplest form, the thrust T can be computed solely by means of a throttle coefficient, δ_T, as

$$T = \delta_T \times T_{max}. \tag{5}$$

A solution such as this one, however, leaves the propulsion system totally independent from the remaining disciplines, providing results which rely solely on the engine parameters defined at the start.

In order to develop the system considering more parameters, a general model such as the one described in Stengel [14] is adopted. As such, the thrust force is broken into its dimensionless and reference factors,

$$T = C_T(V, \delta_T)\frac{S\rho^2}{2}\ , \tag{6}$$

and the dimensionless factor C_T is defined as a function of speed, V, and the throttle coefficient, δ_T, as well as three empirical coefficients,

$$C_T = (k_0 + k_1 V^\eta)\delta_T\ , \tag{7}$$

where S is the total reference area, ρ the atmospheric density, k_0 is the maximum-throttle thrust coefficient at $V = 0$, k_1 is a measure of the speed weighting, and η is a parameter used to describe the engine type. These three coefficients will also be important in order to define the relevant derivatives for the C_T factor.

2.6. Trajectory Approach

The adopted approach to perform trajectory control optimization will consist of breaking down the mission profile into a prescribed number of flight phases (multipoint approach). Only fully-developed situations will be considered in each of the points of the analysis, and these are parameterized into three factors, as illustrated in fig.5.

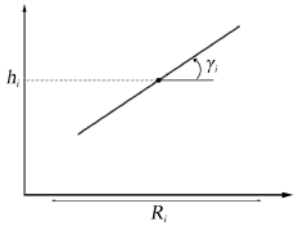

Figure 5: Generic trajectory point.

These factors are the flight path angle, γ_i, altitude, h_i, and ground distance covered, R_i, of the i-th point. Different constraints may be applied to the different points in order to define the trajectory phases in which to perform control optimization. In essence, for each of the trajectories, the model is optimized for a cruise situation, and then the control variables are optimized to other conditions representative of different flight phases.

3. Implementation

3.1. Propulsion

The main characteristics of the propulsive force must be defined; namely its point of application, orientation and magnitude. The two former parameters will be discussed first.

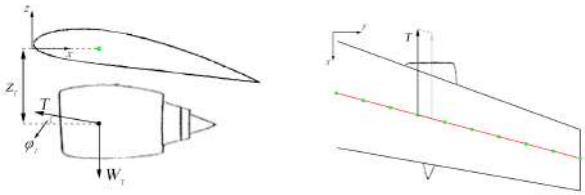

((a)) Side view. ((b)) Top view.

Figure 6: Application of the propulsive force.

Following the diagrams x, y, z defined in fig. 6, several details regarding the application of the thrust force can be defined:

- The force is parallel to the incoming flow, meaning only the aforementioned ϕ_T needs to be defined (i.e. there will be no component in the y-direction). For the sake of simplicity, this angle will be considered null in this work: $(\phi_T = 0)$;
- As a simplification, it may be considered that the force will be applied on one of the nodes of the mesh (denoted in green). Doing so simplifies transferring the force to the structure proper;
- When applying the engine force, a vertical component must be added to represent the weight of the engine. Both this weight and thrust are applied at the same location;
- The vertical distance at which the force will be applied w.r.t. the wing (z_t) will be defined as half of the engine's diameter.

Regarding the magnitude of the propulsive force, the three previously mentioned empirical factors, (k_0, k_1 and η) define the type of engine the model will emulate. Referring once again to Stengel [14], the following assumptions are made

$$\begin{cases} k_0 = 0 \\ \eta = -3 \end{cases} . \tag{8}$$

For all mentioned idealized models k_0 is considered to be 0. Furthermore, setting this value for η describes a constant power setting, representative of high propulsive efficiency systems such as high-bypass turbofans and turboprop coupled to a propeller.

The k_1 parameter will be used to fit the model to specific engines. As a default setting, the values from a specific aircraft will be used: the *B777-300*. As such, for purposes of defining k_1, the values from the *GE90* turbofan will be considered - an engine commonly paired with this aircraft.

Fig. 7 sums up the data flow in this discipline.

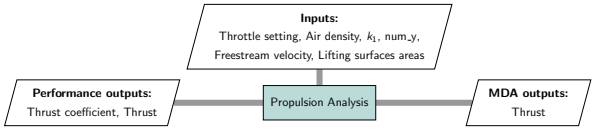

Figure 7: Inputs and outputs of the propulsion analysis.

3.2. Trajectory Control Optimization

The baseline mission profile is that of a cruise condition situation. Within the established framework , this case will consist of a single trajectory point optimization process, with the following conditions

$$\begin{cases} \gamma_1 = 0^o \\ h_1 = 10700m \\ R_1 = 11 \times 10^6 m \end{cases} , \tag{9}$$

where h_1 and R_1 are the cruise altitude and maximum range of the *B777-300*, respectively [15].

Once the optimized aircraft has been computed, its control variables are optimized for a different flight condition, as proof of concept of the approach. Namely, the descent phase will be optimized upon, as illustrated in fig. 8.

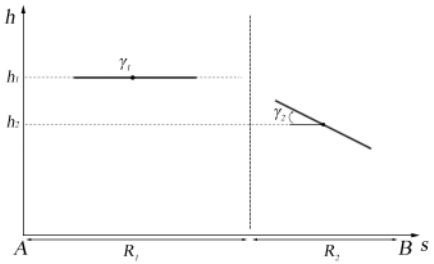

Figure 8: Two point mission profile with cruise and descent.

For the descent different conditions are enforced,

$$\begin{cases} \gamma_2 = -3^o \\ h_2 = 5350m \\ R_2 = 204 \times 10^5 m \end{cases} , \tag{10}$$

where γ_2 is a common-place rule for determining rate of descent [16], h_2 is half of the cruise altitude and R_2 is a direct consequence of descending at a steady -3^o from h_1 to sea level.

3.3. MDO Elements

The fundamental pieces of the optimization problems we will be solving are now established. The design variables can be synthesized as:

- Aerodynamics: angle-of-attack (α), twist distribution$(\theta(y))$ for both wing (w) and tail (t);

- Propulsion: throttle setting (δ_T);
- Structures: spar thickness distribution ($t(y)$) on the wing (w);
- Trajectory: flight path angle (γ);
- Aerostructural: wing span (b_w).

These variables will be constrained to the following ranges,

$$\begin{cases} -15^{\text{o}} \leq \alpha \leq +15^{\text{o}} \\ -15^{\text{o}} \leq \theta_w,\, \theta_t \leq +15^{\text{o}} \\ 0 \leq \delta_T \leq 1 \\ 50 \leq b_w \leq 70m \\ 0.01 \leq t_w \leq 0.05m \end{cases} . \tag{11}$$

The boundaries for the angular variables arise from the small angle approximations assumed in the development of the aerodynamic model. The throttling variable is a percentile. The wingspan boundaries are based on the span of the original aircraft [15]. Lastly, the boundaries for the thickness of the spars have been defined so the final weight of the aircraft resembles that of the original aircraft. To this end, the operating empty weight (OEW) is used as a reference. From [15], the OEW should be close to $1.7 \times 10^5 kg$. One important note regarding the implementation of the spar thicknesses and twist (for the wing) is that these distributions are defined by a spline. Essentially, rather than defining the twist and spar thickness at every control point of the structure as a design variable, a desired number of control points for these two distributions is defined and a B-spline curve is derived from these.

As for the constraints, auxiliary variables have been defined to describe two of the trimming conditions laid out in 2.2, namely

$$\begin{cases} L\_\text{eq}\_W = cos(\gamma) - \frac{L}{W} - \frac{Tsin(\alpha)}{W} = 0 \\ T\_\text{eq}\_D = sin(\gamma) + \frac{D}{W} - \frac{Tcos(\alpha)}{W} = 0 \end{cases} . \tag{12}$$

Since the model assumes symmetry across the xz-plane, both the yaw and roll are null by construction. the tool computes the pitch moment, meaning we need only to enforce

$$C_{M_y} = 0\,. \tag{13}$$

Additionally, the non-failure of the structural elements is enforced by means of a Von-Mises criterion,

$$\text{Failure} = 2\frac{\sigma_{VM}}{\sigma_y} - 1 \leq 0\,, \tag{14}$$

where σ_{VM} is the Von-Mises stress and σ_y is the material yield strength. The multiplicative factor in eq. 14 arises from the safety factor of 2.0 considered in this work. A constraint aggregation method based on the Kreisselmeier-Steinhauser equation [17] is employed. This way, only a single failure constraint needs to be applied, rather than one for each on the elements.

Lastly, a strictly computational constraint is set to ensure that the optimizer maintains the tubular structure geometrically feasible, in the form of

$$\text{Intersection} = \text{Thickness} - \text{Radius} \leq 0\,. \tag{15}$$

As discussed previously, the metric to be minimized is the amount of fuel consumed in a prescribed mission. Because the propulsive force is explicitly computed for each flight phase, we may define the objective function as

$$m_{\text{fuel}} = \sum_{i=1}^{N} TSFC \frac{R_i}{V_i} T_i\,, \tag{16}$$

where the mission profile has been sectioned into N phases, and $TSFC_i$, R_i, V_i and T_i are respectively the thrust-specific fuel consumption (in $kg/N/s$ units), covered distance, speed and thrust of each phase.

4. Results

4.1. Initial Setup

A simple mesh convergence study was performed first, wherein a single iteration of the MDA process was carried out with a progressively finer mesh. The relative change in the performance metric was used to evaluate the convergence.

Table 1: x-direction.

num_x	$\delta(m_{\text{fuel}})$ (%)
2	-
3	-0.00852
5	-0.00413
7	-0.00172
9	-0.00095

Table 2: y-direction.

num_y	$\delta(m_{\text{fuel}})$ (%)
5	-
7	-2.57
...	...
21	-0.0387
23	-0.00851

A criterion of $\delta(m_{\text{fuel}}) \leq 0.01\%$ was applied, meaning a $[3 \times 23]$ grid was employed.

Additionally, the mechanical properties of Aluminum-7075 are considered for the spars of both the wing and tail; and the following group of parameters.

Table 3: Cruise flight conditions.

Parameter	Value
M	0.84
$h(m)$	10.7×10^3
$\rho(kg/m^3)$	0.38
Range (m)	11×10^6
$W_0(kg)$	1.125×10^5
TSFC $(kg/N/s)$	1.54×10^{-5}

Table 4: Tail parameters.

Parameter	Value
$b_t(m)$	24.22
λ_t	0.118
$l_t(m)$	0.05

Table 5: Numerical Parameters.

Parameter	Value
Iterative tolerance	10^{-7}
Optimizer tolerance	10^{-3}

W_0 is a parameter which factors for rest of the operating empty weight apart from the weight of the wing and tail structures which will are computed. The tail parameters were obtained by performing an optimization problem similar to the one which will be discussed in section4.3, starting from a symmetrical rectangular surface. These values are not considered as design variables as it was observed that doing so greatly increased the problem's complexity for minimal objective function gains. The iterative tolerance applies to the MDA analysis at each design point, whilst the optimizer tolerance applies to the overarching constraints of the problem (for example, the trimming conditions).

4.2. Aerodynamic & Propulsion Optimization

The first situation consists of single-point optimization considering the aerodynamic and propulsive systems in a cruise setting - an aeropropulsive (AP) problem. This optimization problem is defined as

$$\begin{array}{ll} \text{minimize} & \text{Fuelburn} \\ \text{with respect to} & \alpha, \gamma, \theta_t, \theta_w, \delta_T, b_w \\ \text{subject to} & L\_\text{equals}\_W = 0 \\ & T\_\text{equals}\_D = 0 \\ & C_{M_y} = 0 \\ & \gamma = 0 \end{array}, \tag{17}$$

where all constraints and design variables are considered except for those pertaining exclusively to the wing structure: the spar thicknesses and their failure.

A study similar to the one described in the previous section was carried out to determine the optimal number of points with which to define the B-spline for the wing twist.

Table 6: Convergence in m_{fuel}.

B-spline points	$\delta(m_{\text{fuel}})$ (%)
2	-0.225
3	-0.00260
4	-0.00104

Applying the same criterion, a 3-point curve was chosen.

Table 7 lists the initial values and allowed ranges for the design variables (DV).

Table 7: Initial DV values and ranges (AP).

DV	Initial value	Range
$\alpha(^\circ)$	5	$[-15, +15]$
$\gamma(^\circ)$	2	$[-15, +15]$
$\theta_t(^\circ)$	-5	$[-15, +15]$
$\theta_w(^\circ)$	$(-3.75, 1.5, 7)$	$[-15, +15]$
δ_T	0	$[0, 1]$
$b_w(m)$	60	$[50, 70]$

All conditions have been defined, and the optimization process may now be carried out. Table 8 lists the final values for the design variables, constraints and objective function. Fig. 9 is a full plot of the obtained configuration.

Table 8: Final values for AP optimization.

DV	Final value
$\alpha(^\circ)$	5.09
$\gamma(^\circ)$	0
$\theta_t(^\circ)$	-12.8
$\theta_w(^\circ)$	$(-3.81, 2.08, 11.2)$
δ_T	0.220
$b_w(m)$	61.6
L_equals_W	-1.68×10^{-5}
T_equals_D	4.82×10^{-6}
C_{M_y}	-1.01×10^{-5}
Fuelburn (kg)	130193.0

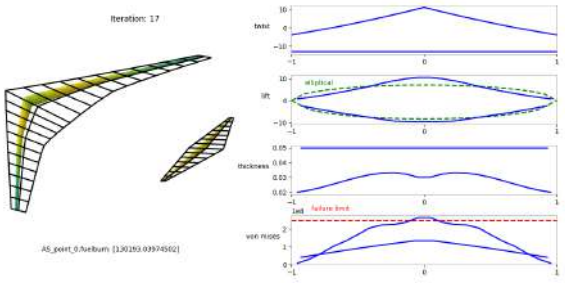

Figure 9: Configuration for the AP optimization.

This optimization process elapsed 18 iterations, and was concluded in $127.16s$. The process was successful, as all constraints are met (within their designated threshold) and all design variables concluded within their established ranges.

The obtained wingspan ($61.6m$) is close to that of the *B777-300* ($60.9m$, with a relative error of 1.15%). Also, assuming a jet fuel density of around

$800kg/m^3$, the mass of fuel computed translates to

$$V_{\text{Fuelburn}} = \frac{130193}{800} = 162.7413m^3 = 162741.3l,$$

which is 4.93% lower the original aircraft maximum fuel capacity. This is adequate, since maximum range was considered and no fuel reserves were included.

In fig. 9 it can be observed that the wing structure experienced failure (bottom-right plot). This was to be expected, since this constraint was not enforced. Also in this figure, the twist plot displays a nearly linear progression across the wingspan (top-right plot), even though a 3-point B-spline curve was utilized. This is congruent with the small variations described in table 6, suggesting the optimized twist distribution is accurately described with just 1 or 2 curve points. Still in the same figure, the middle-right plot exhibits one of the hallmarks of MDO versus sequential optimization in aircraft design. Sequential optimization yields elliptic lift distributions [18], and the lift distribution for the computed wing strays away from the green dashed line.

4.3. Aerostructural & Propulsion Optimization

Now, the structural design variables and constraints are added - an aerostructural propulsive (ASP) problem. The optimization problem becomes

$$\begin{array}{ll} \text{minimize} & \text{Fuelburn} \\ \text{with respect to} & \alpha, \gamma, \theta_t, \theta_w, \delta_T, b_w, t_w \\ \text{subject to} & L\_\text{equals}\_W = 0 \\ & T\_\text{equals}\_D = 0 \\ & C_{M_y} = 0 \\ & \gamma = 0 \\ & \text{Failure} \leq 0 \\ & \text{Intersection} \leq 0 \end{array} \quad . \tag{18}$$

The wing spar thickness distribution is another parameter defined by a B-spline curve. As such, a similar study was performed to determine the number of points to be considered.

Table 9: Convergence in m_{fuel}.

B-spline points	$\delta(m_{\text{fuel}})$ (%)
2	+0.0250
3	−0.0386
4	+0.00581
5	−0.00407

The same criterion was applied, meaning a 4-point curve. Table 10 lists the initial values and ranges for the design variables.

Table 10: Initial DV values and ranges (ASP).

DV	Initial value	Range
$\alpha(^\circ)$	5	$[-15, +15]$
$\gamma(^\circ)$	2	$[-15, +15]$
$\theta_w(^\circ)$	$(-3.75, 1.5, 7)$	$[-15, +15]$
$\theta_t(^\circ)$	-5	$[-15, +15]$
δ_T	0	$[0, 1]$
$b_w(m)$	60	$[50, 70]$
$t_w(m)$	$(0.02, 0.0233, 0.04, 0.03)$	$[0.01, 0.05]$

Once again, table 11 lists the final values for the problem parameters, and fig. 10 displays a full plot of the fully-optimized cruise configuration.

Table 11: Final values for ASP optimization.

DV	Final value
$\alpha(^\circ)$	5.13
$\gamma(^\circ)$	0
$\theta_w(^\circ)$	$(-3.82, 2.06, 11.03)$
$\theta_t(^\circ)$	-12.8
δ_T	0.220
$b_w(m)$	61.5
$t_w(m)$	$(0.0295, 0.0295, 0.0440, 0.0325)$
L_equals_W	-4.88×10^{-5}
T_equals_D	6.15×10^{-6}
C_{M_y}	-1.15×10^{-4}
Failure	-1.86×10^{-5}
Intersection	$(-0.209 \sim -0.933)$
Fuelburn (kg)	129872.9

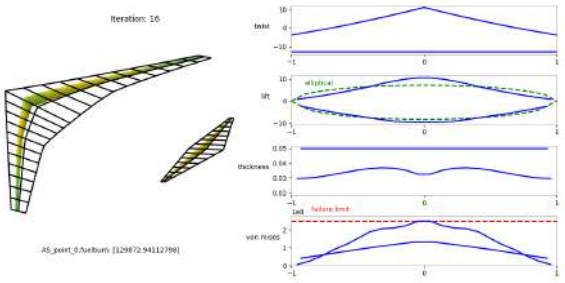

Figure 10: Configuration for the ASP optimization.

This optimization was carried out in 17 iterations, over a time period of 138.59s. Once again, all of the constraints have been met, and all design variables remained within the established values. This final solution is very similar to the previous one, as can be seen from the values in table 11. A relative decrease of 0.246% has been attained in the amount of fuel spent, at the cost of a 8.99% increase in computation time. It should be noted that in the AP optimization process carried out in the previous section the structural computations were still performed, the difference between both cases is

solely that all design variables and constraints pertaining exclusively to the discipline were omitted in the previous process. The computational cost gap between both processes would certainly be greater if this were not the case. Both new design variables as well as new constraints were added, meaning there was no reason to necessarily expect either a better or worse solution. Some of the trends pointed out in the previous analysis are still present, such as the non-elliptical lift distribution and the nearly linear twist distribution. The failure constraint is also met.

Lastly, now that the wing structure has been involved in the optimization process, a comparison may be made between the computed operating empty weight and that of the original $B777-300$. The structural masses computed in this optimization process were $43632.3kg$ and $10558.3kg$ for the wing and tail, respectively. Adding these to the W_0 parameter described in table 3 yields

$$W_0 + W_{\mathrm{w}} + W_{\mathrm{t}} = 166690.5kg. \tag{19}$$

This is another good fit to the original value of $160500kg$ [15], with a relative error of 3.86%.

4.4. Descent Control Optimization

Now that the cruise-optimized aircraft configuration has been computed, the last step is to optimize its control variables to the second flight phase, the descent. The descent control optimization problem takes the following form

$$\begin{array}{ll} \text{minimize} & \text{Fuelburn} \\ \text{with respect to} & \alpha, \gamma, \theta_t, \delta_T \\ \text{subject to} & L\_\text{equals}\_W = 0 \\ & T\_\text{equals}\_D = 0 \\ & C_{M_y} = 0 \\ & \gamma = -3^{\mathrm{o}} \end{array}, \tag{20}$$

where all non-control variables and constraints, i.e. any variables which would change the shape and/or structure of the established wing, have been omitted. The initial (and constant) values for these absent parameters will be those obtained from the ASP optimization, listed in table 11. The atmospheric properties have also been changed as function of the new altitude, namely

$$\begin{cases} \rho_2 = 0.709kg/m^3 \\ c_2 = 319.1m/s \\ M_2 = 0.63 \end{cases}, \tag{21}$$

where c_2 is the new speed of sound.

Table 12 lists the final values for the control variables.

Table 12: Final values for the descent.

CV	Final value
$\alpha(^{\mathrm{o}})$	-0.186
$\gamma(^{\mathrm{o}})$	-3
$\theta_t(^{\mathrm{o}})$	-2.13
δ_T	0.0510
L_equals_W	-4.51×10^{-4}
T_equals_D	-6.58×10^{-5}
C_{M_y}	-2.78×10^{-5}
Fuelburn (kg)	668.9

This optimization process elapsed 7 iterations over the course of $72.96s$, which indicates a significantly lower computational load than the previous cases. This was to be expected since the control optimization problem was, initial conditions apart, strictly simpler than any of the previously discussed problems.

This approach, and therefore these results, cannot be completely separated from the optimization process which we performed previously, since we are attributing an additional amount of fuel necessary for the descent step which was not technically considered previously.

However, the ratio between the two fuel masses showcases why this is a reasonable approximation:

$$\frac{\text{Fuelburn}_{\text{Descent}}}{\text{Fuelburn}_{\text{Cruise}}} = \frac{668.9}{129872.9} = 0.0052. \tag{22}$$

The decision to optimize upon the control of the descent phase in specific was deliberate, as this phase incurs a relatively low fuel consumption when compared to other commonly defined flight phases.

This process shows that the obtained design can handle descent stipulations, providing the control variable values that should employed. As with the previous optimizations, all constraints have been met, including the control variable boundaries.

5. Conclusions

In this work, existing aerostructural multidisciplinary optimization code was expanded upon by implementing a propulsive system. MDO was successfully performed considering the three disciplines and all their respective parameters for a cruise situation. Several of the values obtained in the final aircraft design closely resembled those of the original aircraft which was to be emulated, the $B777-300$. These included the empty operating weight, wingspan and amount of fuel consumed in a maximum range situation. Optimization of the control variables of the system was also successfully carried out for performance on a different flight phase, the descent.

Overall, the final code managed to accomplish nearly everything it was expected to, though there are still several aspects in which it can be improved.

Regarding the propulsive force placement, the engine position in the span could have been parameterized, and acted as a design variable. This could be accomplished either as a discrete variable, assuming that the force would always be applied at a structural node (similar to what was done in this work); or as a continuous parameter, paired with a load/moment transfer scheme.

It could also be interesting to optimize the control variables upon more flight conditions. Because, however, the initial cruise-only optimization becomes less and less accurate the more of these are tacked on, an important improvement to this code would be to implement a complete multipoint optimization scheme. This way, all of the design variables and all of the stipulated flight conditions would be simultaneously considered, and the process would yield the control values for all stages in tandem with an aircraft optimized upon all of the mission phases.

References

[1] Hyoungjin Kim, David Harding, David T. Gronstal, May-Fun Liou, and Meng-Sing Liou. Design of the hybrid wing body with nacelle: N3-x propulsion-airframe configuration. *34th AIAA Applied Aerodynamics Conference*, June 2016. DOI: 10.2514/6.2016-3875.

[2] Ian R. Chittick and Joaquim R. R. A. Martins. An asymmetric suboptimization approach to aerostructural optimization. *Optimization and Engineering*, 10(1):133–152, March 2009.

[3] John P. Jasa, John T. Hwang, and Joaquim R. R. A. Martins. Open-source coupled aerostructural optimization using python. *Structural and Multidisciplinary Optimization*, pages 1–13, January 2018. doi: 10.1007/s00158-018-1912-8.

[4] Joaquim R. R. A. Martins. A coupled-adjoint method for high-fidelity aero-structural optimization. Master's thesis, stanford university, 2002.

[5] Antoine DeBlois and Mohammed Abdo. Multifidelity multidisciplinary design optimization of metallic and composite regional and business jets. *13th AIAA/ISSMO Multidisciplinary Analysis Optimization Conference*, 2010.

[6] Robert D Falck and Justin S Gray. Optimal control within the context of multidisciplinary design, analysis, and optimization. In *AIAA Scitech 2019 Forum*, page 0976, 2019.

[7] Justin Gray, Kenneth Moore, and Bret Naylor. Openmdao: An open source framework for multidisciplinary analysis and optimization. In *13th AIAA/ISSMO Multidisciplinary Analysis Optimization Conference*, page 9101, 2010.

[8] J. R. R. A. Martins and Andrew B. Lambe. Multidisciplinary design optimization: A survey of architectures. *AIAA Journal*, September 2013. DOI: 10.2514/1.J051895.

[9] Andrew B. Lambe and Joaquim R. R. A. Martins. Extensions to the design structure matrix for the description of multidisciplinary design, analysis, and optimization processes. *Structural and Multidisciplinary Optimization*, 46(2):273–284, January 2012. doi:10.1007/s00158-012-0763-y.

[10] A. C. Marta. Aircraft optimal design - course notes. IST, 2018.

[11] Paul T. Boggs and Jon W. Tolle. Sequential quadratic programming. *Acta Numerica*, 1995.

[12] John T. Hwang and Joaquim R. R. A. Martins. A computational architecture for coupling heterogeneous numerical models and computing coupled derivatives. *ACM TOMS*, 44, 2018.

[13] John D. Anderson. *Fundamentals of Aerodynamics*. McGraw-Hill, 5th edition, 2010.

[14] Robert F. Stengel. *Flight Dynamics*. Princeton University Press, 5th edition, 2004.

[15] Boeing 777 specs, what makes this giant twin work? http://www.modernairliners.com/boeing-777/boeing-777-specs/ [Accessed 27 June 2019].

[16] Charles R. Moren. Pilots, airplanes, and the tangent of three (3) degrees. The PUMAS Collection, December 1999.

[17] JRRA Martins and Nicholas MK Poon. On structural optimization using constraint aggregation. In *VI World Congress on Structural and Multidisciplinary Optimization WCSMO6, Rio de Janeiro, Brasil*, 2005.

[18] Joaquim R. R. A. Martins. Multidisciplinary design optimization. Presentation at 7th International Fab Lab Forum and Symposium on Digital Fabrication, August 2011.